Fluids of platelike particles near a hard wall

L. Harnau and S. Dietrich
Max-Planck-Institut für Metallforschung, Heisenbergstrasse 1, D-70569 Stuttgart, Germany
and Institut für Theoretische und Angewandte Physik, Universität Stuttgart, D-70550 Stuttgart, Germany
(Received 26 July 2001; published 16 January 2002)

Fluids consisting of hard platelike particles near a hard wall are investigated using density-functional theory. The density and orientational profiles, as well as the surface tension and the excess coverage, are determined and compared with those of a fluid of rodlike particles. Even for low densities, slight orientational packing effects are found for the platelet fluid due to larger intermolecular interactions between platelets as compared with those between rods. A net depletion of platelets near the wall is exhibited by the excess coverage, whereas a change of sign of the excess coverage of hard-rod fluids is found upon increasing the bulk density.

DOI: 10.1103/PhysRevE.65.021505 PACS number(s): 82.70.Dd, 61.20.−p, 61.30.Gd

I. INTRODUCTION

While many theoretical studies have been devoted to the understanding of the behavior of elongated hard colloidal particles near a hard wall (see, e.g., Refs. [1–8]), suspensions of disc-shaped hard particles near a hard wall have not yet been investigated. One reason is that experimentally a corresponding hard platelet model system, i.e., consisting of particles with a short-range repulsive interaction has been lacking until recently. From a theoretical point of view, the platelet fluid problem appears to be difficult because the Onsager approach of truncating the corresponding equation of state at second order, which is valid for thin rodlike particles, cannot be justified for platelets [9]. Recently, preparation methods have been developed for other types of platelet suspensions, which may indeed serve as model systems of hard colloidal platelets [10–12]. In the present paper we use density-functional theory (Sec. II) to study the positional and orientational order as well as the surface tension and excess coverage of thin-hard platelets near a hard wall (Sec. III). Particularly, the density functional used here includes a third-order density term, which is not present in the Onsager second virial approximation.

II. MODEL AND DENSITY-FUNCTIONAL THEORY

We consider an inhomogeneous fluid consisting of thin platelets of radius R in a container of volume V. The platelets are taken to be hard discs without attractive interactions. The number density of the centers of mass of the platelets at a point $\mathbf{r}$ with an orientation $\omega=(\theta,\phi)$ of the normal of the platelets (see Fig. 1) is denoted by $\rho(\mathbf{r},\omega)$. The equilibrium density profile of the inhomogeneous liquid under the influence of an external potential $V(\mathbf{r},\omega)$ minimizes the grand potential functional [13]:

$$\Omega[\rho(\mathbf{r},\omega)]=\int d\mathbf{r}\,d\omega\rho(\mathbf{r},\omega)[k_BT(\ln[4\pi\Lambda^3\rho(\mathbf{r},\omega)]-1) - \mu+V(\mathbf{r},\omega)]+F_{\rm ex}[\rho(\mathbf{r},\omega)], \tag{2.1}$$

where Λ is the thermal de Broglie wavelength and μ is the chemical potential. We express the excess free energy functional $F_{\rm ex}[\rho(\mathbf{r},\omega)]$ as an integral over all spatial and orientational degrees of freedom for the corresponding local free-energy density $f_{\rm ex}[\rho=\rho(\mathbf{r},\omega)]$ of the fluid

$$F_{\rm ex}[\rho(\mathbf{r},\omega)]=\int d\mathbf{r}_1 d\omega_1 d\mathbf{r}_2 d\omega_2 w(\mathbf{r}_1,\omega_1,\omega_2) \times\rho(\mathbf{r}_1,\omega_1)f_{\rm ex}[\rho(\mathbf{r}_2,\omega_2)], \tag{2.2}$$

with

$$f_{\rm ex}(\rho)=4\pi^2\left[\sqrt{2}R^3\rho+\frac{4\pi^2}{3}R^6\rho^2\right]k_BT. \tag{2.3}$$

This functional incorporates fluid correlations via a weight function $w(\mathbf{r}_1,\mathbf{r}_2,\omega_1,\omega_2)$ and bulk thermodynamics via a recently developed equation of state of thin platelets [14]

$$p_b=-\left(\frac{\partial\Omega}{\partial V}\right)_{T,\mu}=\rho_b\left(1+\sqrt{2}\pi R^3\rho_b+\frac{2\pi^2}{3}R^6\rho_b^2\right)k_BT, \tag{2.4}$$

where $\rho_b=V^{-1}\int dr\int d\omega\rho(\mathbf{r},\omega)$ is the number density of the homogeneous and isotropic bulk fluid. We note that the resulting excess free-energy functional $F_{\rm ex}[\rho(\mathbf{r},\omega)]$ includes a cubic term of the density, which is not present in the Onsager second virial approximation [9]

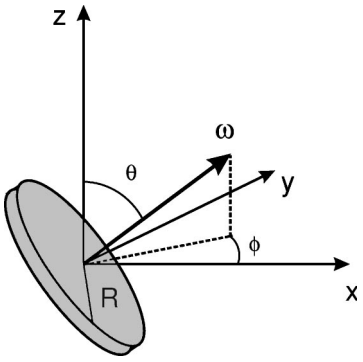

FIG. 1. The polar angle θ and the azimuthal angle ϕ of the normal ω of a thin platelet of radius R with its center of mass located at $\mathbf{r}=(0,0,0)$.

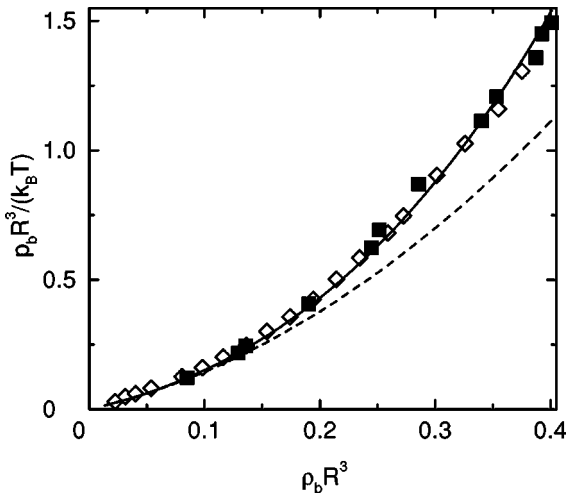

FIG. 2. Equation of state of thin platelets as obtained from Eq. (2.4) (solid line), and from computer simulations (squares [15] and diamonds [16]). The dashed line follows from Eq. (2.4) by omitting the cubic term $\sim\rho_b^3$.

$$f_{\rm ex}^{\rm rod}(\rho)=\pi^2 DL^2\rho\, k_B T \tag{2.5}$$

used in the description of thin rods of length L and diameter D near surfaces (see, e.g., Refs. [2], [3] and [5]). The necessity for including this higher-order density term already follows from comparing the ensuing bulk pressure [Eq. (2.4)] with corresponding simulation data [15,16] (see Fig. 2). Fluids consisting of thin platelets exhibit an isotropic and a nematic phase with no other liquid-crystalline phases, such as a columnar phase, observed [15]. The isotropic-nematic (IN) transition is first order with coexistence densities at $\rho_{bI}R^3=0.46$ and $\rho_{bN}R^3=0.5$ according to a computer simulation [17].

Minimization of Ω with respect to $\rho(\mathbf{r},\omega)$ leads to the following integral equation for the equilibrium density distribution:

$$\begin{aligned} k_B T\ln[4\pi\Lambda^3\rho(\mathbf{r},\omega)] &= \mu - V(\mathbf{r},\omega) - 8\pi^2 R^3\int d\mathbf{r}_1 d\omega_1 \rho(r_1,\omega_1) \\ &\times w(\mathbf{r},\mathbf{r}_1,\omega,\omega_1)[\sqrt{2}+\tfrac{2}{3}\pi^2 R^3[2\rho(\mathbf{r},\omega) \\ &+\rho(\mathbf{r}_1,\omega_1)]]k_B T. \end{aligned} \tag{2.6}$$

We have solved this equation numerically for a given chemical-potential μ and a given external-field $V(\mathbf{r},\omega)$. The weight function is taken to be a function of the relative positions $\mathbf{r}_{12}=\mathbf{r}_1-\mathbf{r}_2$, and is normalized so that $\int d\mathbf{r}_{12}d\omega_2 w(\mathbf{r}_{12},\omega_1,\omega_2)=1$. In this paper, the weight function is given by the Mayer function, except for the normalization. The Mayer function equals -1 if the platelets overlap and is zero otherwise. Two platelets, separated by a distance $\mathbf{r}_{12}$, intersect if the inequality

$$\begin{aligned} |\mathbf{r}_{12}\cdot(\boldsymbol{\omega}_1\times\boldsymbol{\omega}_2)| &< \sqrt{R^2\sin\gamma_{12}^2-(\mathbf{r}_2\cdot\omega_2)^2} \\ &+\sqrt{R^2\sin\gamma_{12}^2-(\mathbf{r}_{12}\cdot\boldsymbol{\omega}_1)^2}, \end{aligned} \tag{2.7}$$

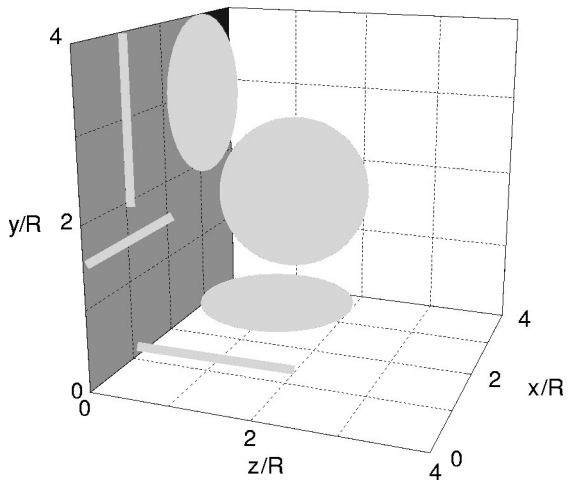

FIG. 3. The two systems under consideration consist of fluids of monodisperse thin platelets of radius R and thin rods of length $L=2R$ in contact with a planar hard wall at $z=0$. Particles very close to the wall must adopt nearly a fully parallel alignment. Here, the three principal directions are shown.

with $\boldsymbol{\omega}_j=(\sin\theta_j\cos\phi_j,\sin\theta_j\sin\phi_j\cos\theta_j)$, $j=1,\ 2,$ is fulfilled. γ_{12} is the angle between the normals $\boldsymbol{\omega}_1$ and $\boldsymbol{\omega}_2$ of two platelets. Equation (2.7) has been derived and is amply documented in Ref. [15]. In practice, first the weight function is calculated by testing Eq. (2.7) and is stored for all required values of $(\mathbf{r}_{12},\omega_1,\omega_2)$.

Thereafter, the integral equation (2.6) is solved using a Picard scheme with retardation.

III. PLATELETS AND RODS NEAR A HARD WALL

For model systems of hard particles near a hard wall at $z=0$ (see Fig. 3), apart from a possible surface freezing at high densities, nonuniformities of the density occur only in the z direction, so that $\rho(\mathbf{r},\omega)=\rho(z,\theta,\phi)$. Figure 4 displays the calculated platelet density profile for the bulk density $\rho_b R^3=0.2$. The calculations render $\rho(z,\theta,\phi)$ to be independent of the azimuthal angle ϕ for this density, i.e., there is no biaxial order emerging at the wall like for hard rods at high densities [6–8]. For $z<R$, orientations with large θ values are forbidden so that the density profile has a discontinuity along the line $z_{\rm min}=R\sin\theta$. There is a pronounced increase of the density near the surface. Moreover, slight packing effects are visible through oscillations at $z\approx 2R$. For comparison, Fig. 5 displays the density profile of thin rods near a hard wall calculated from Eqs. (2.1), (2.2), and (2.5). Fluids consisting of thin rods exhibit an isotropic-nematic transition with coexistence densities at $\rho_{bI}DL^2=3.3$ and $\rho_{bN}DL^2=4.49$ according to the Onsager approach [9]. The bulk density has been fixed such that the second virial coefficient of the equation of state of thin platelets [see Eq. (2.4)] and of the equation of state of thin rods,

$$p_b^{\rm rod}=\rho_b(1+\tfrac{\pi}{4}DL^2\rho_b)k_B T, \tag{3.1}$$

are equal in units of R^3 and DL^2, respectively. Due to the presence of the wall $\rho(z,\theta,\phi)$ vanishes if $z<z_{\rm min}$

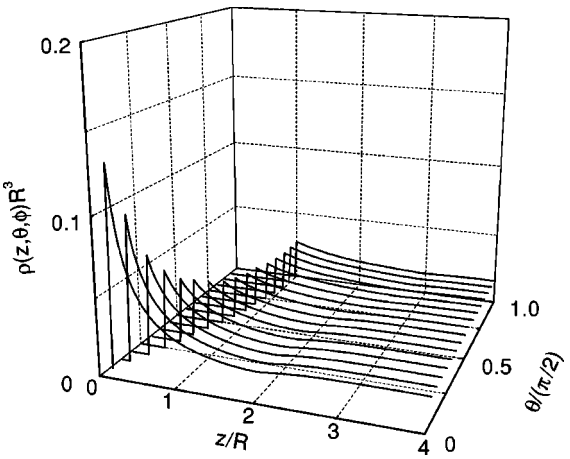

FIG. 4. Center-of-mass density profile $\rho(z,\theta,\phi)R^3$ of thin platelets near a hard wall for various angles θ of the platelet normals relative to the surface normal. The density profile is independent of the azimuthal angle ϕ. At small distances z from the wall, large values of θ are forbidden due to overlap. Therefore, the profile is exactly zero if $z<z_{\min}=R\sin\theta$. The bulk density is fixed to $\rho_b R^3=0.2$.

$=(L/2)\cos\theta$. Hence, in terms of the normals of the platelets and the normals of the rods along their main axis of symmetry the preferred orientation of rods near a hard wall is perpendicular to the preferential orientation of the platelets. This means that in both cases, the main body of the particles tends to lie parallel to the wall (see Fig. 3). In agreement with earlier calculations [5], for rods, no packing effects are visible because of the relatively smaller intermolecular interactions between rods as compared with those between platelets. (For thin rods, the intersection volume is pointlike, whereas for discs it is similar to a line segment.)

We have tested successfully the accuracy of the numerical calculations by comparing our results for the profiles with the pressure sum rule

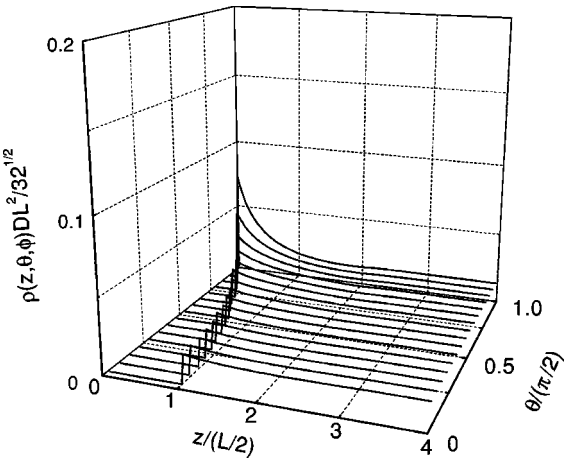

FIG. 5. Center-of-mass density profile $\rho(z,\theta,\phi)DL^2/\sqrt{32}$ of thin rods ($L/D\to\infty$) near a hard wall for the bulk density $\rho_b DL^2/\sqrt{32}=0.2$. The profile is exactly zero if $z<z_{\min}=(L/2)\cos\theta$ due to overlap.

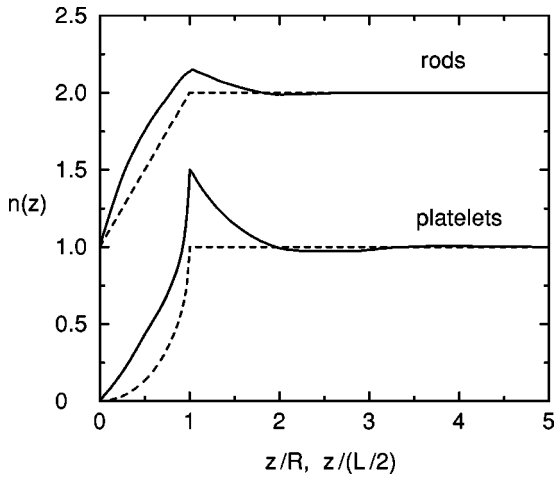

FIG. 6. Normalized, orientationally averaged density profile $n(z)$ for platelets (lower-solid curve) and rods (upper-solid curve) in contact with a hard wall for the same bulk density as in Figs. 4 and 5. The length L of the rods and the diameter of the platelets $2R$ are taken to be the same. The dashed lines represent the results for an ideal gas of platelets and rods, respectively. The upper curves are shifted by one.

$$p_b=k_BT\int_0^{2\pi}d\phi\int_0^{\pi}d\theta\sin\theta\rho(z_{\min}\theta,\phi),\qquad(3.2)$$

and we found good agreement. Equation (3.2) is an extension of the pressure sum rule of a hard-sphere fluid near a wall (see, e.g., Ref. [18]). The weighted density-functional theory guarantees that the wall sum rule is satisfied, provided that the pressure enters through the corresponding bulk equation of state.

A set of position-dependent order parameters quantifies the deviation from isotropy of the number density. For a uniaxial density profile, the most general form of $\rho(z,\theta,\phi)$ is independent of ϕ so that one can write

$$\rho(z,\theta)=\sum_{l=0}^{\infty}\frac{2l+1}{2}Q_l(z)P_l[\cos(\theta)],\qquad(3.3)$$

where $P_l[\cos(\theta)]$ are the Legendre polynomials. The normalized, orientationally averaged number density profiles $n(z)=2\pi Q_0(z)/\rho_b$ are displayed in Fig. 6, together with the results for noninteracting platelets and rods. Upon increasing z from the wall the averaged number densities increase and exhibit cusps at $z=R$ for platelets, and at $z=L/2$ for rods, respectively. For rods, the maximum at the cusp is only about 10% above the bulk value, which is essentially reached already for $z=L$. For platelets, the maximum is more pronounced and slight packing effects are visible at larger values of z due to the relatively larger steric interactions between platelets.

The position-dependent uniaxial, relative nematic order parameter $s(z)=Q_2(z)\rho_b/[2\pi Q_0(z)]$ is displayed in Fig. 7. At small values of z, the value of the nematic order parameter reflects the geometric constraints. A platelet (rod) lying very close to the wall must adopt nearly a fully parallel alignment, so that the order parameter reaches the limiting

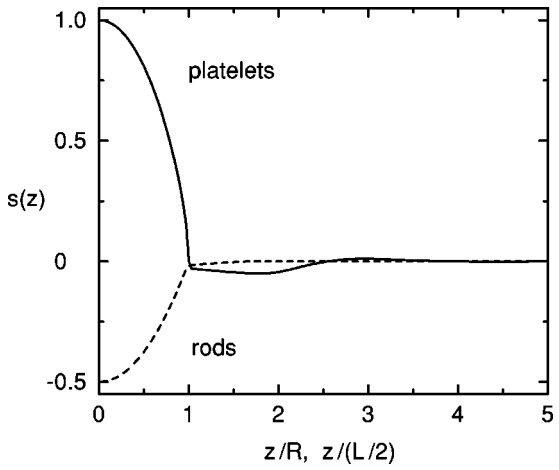

FIG. 7. Relative uniaxial nematic order parameter $s(z)$ for platelets (solid curve) and rods (dashed curve) in contact with a hard wall for the same bulk density as in Figs. 4 and 5. Positive (negative) values of the nematic order parameter indicate that the platelets (rods) are preferentially aligned parallel to the wall.

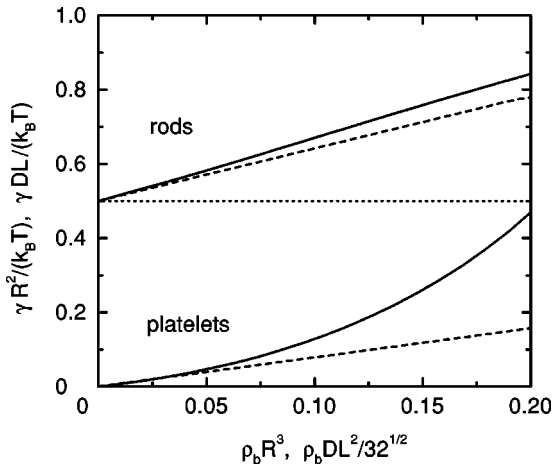

FIG. 8. Surface tension of a fluid consisting of thin hard platelets of radius R (lower-solid curve) and hard rods of length L and diameter D (upper-solid curve, $L/D\to\infty$) near a hard wall. The dashed lines represent the results for an ideal gas of platelets and rods, respectively. The upper curves are shifted by 0.5 (dotted line).

value $1=P_2[\cos(0)]$, $\{-0.5=P_2[\cos(\pi/2)]\}$ there, whereas isotropic orientation at large distances from the wall is characterized by $s(z)=0$. Interestingly, the nematic order parameter for platelets has a minimum at $z\approx 2R$ due to a depletion of platelets parallel to the wall. In other words, a platelet, next to the platelet at $z=R$ with the rim touching the wall (see Fig. 3), is oriented rather parallel than perpendicular to the former.

It is useful to consider not only local but also global properties of a liquid near a surface. There are two global quantities, which are of experimental interest and of interest for simulations: the excess coverage, which is accessible by, e.g., gravimetric measurements; and the surface tension which, for example, is important for contact angles. The surface tension γ is defined via

$$\Omega[\rho(z,\theta,\phi)]=V\omega_b+\gamma S, \tag{3.4}$$

where S is the surface area and $\omega_b=-p_b$ [see Eq. (2.4)] is the bulk grand-canonical potential density. The surface tension depends on the definition of what is denoted as the volume V [19]. We have defined V as the volume of the container with its surface given by the position of the rim of the particles at closest approach so that the region $0<z<z_{\min}$ is part of V. Figure 8 displays the calculated surface tension together with the results for noninteracting platelets and rods. The steric interaction between the particles, which is more pronounced for the platelets, increases the surface tension with increasing density. The results for the rods are in agreement with those obtained in Refs. [3] and [5].

The excess coverage

$$\Gamma=\rho_b\int_0^\infty dz[n(z)-1] \tag{3.5}$$

provides an important overall characterization of the density profiles. Figure 9 summarizes the results for platelets and rods. Repulsive interactions between the platelets and the hard wall lead to a net depletion near the surface ($\Gamma<0$). The excess coverage of rods exhibits a change of sign with increasing density in agreement with recent density functional calculations [6,7] and computer simulations [8].

IV. SUMMARY

We have applied a density-functional theory to fluids consisting of thin-hard platelets and rods in contact with a hard wall. Particles lying very close to the wall must adopt nearly a fully parallel alignment due to interactions with the wall (Fig. 3). The probability of finding a particle touching the wall is increased compared with the bulk (Figs. 4 and 5). A comparison between the rod fluid and the platelet fluid exhibits slight orientational packing effects for the platelet fluid (Fig. 7) and that the increase of the surface tension with

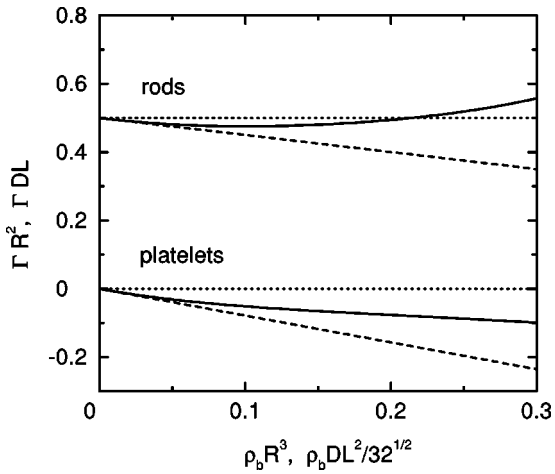

FIG. 9. Excess coverage [see Eq. (3.5)] of a fluid consisting of thin platelets of radius R (lower-solid curve) and rods of length L and diameter D (upper-solid curve, $L/D\to\infty$) near a hard wall. The dashed lines denote the corresponding results for an ideal gas of platelets and rods, respectively. The upper curves are shifted by 0.5.

increasing density is more pronounced for platelets than for rods (Fig. 8) due to larger intermolecular interactions between platelets as compared with those between rods. The calculated excess coverage (Fig. 9) reveals a depletion of platelets close to the wall (Fig. 6), whereas a change of sign of the excess coverage of hard-rod fluids indicate the onset of wetting. Work is currently in progress to study the wetting behavior of platelets at higher densities.

ACKNOWLEDGMENT

L.H. gratefully acknowledges support by the Deutsche Forschungsgemeinschaft.

[1] A. Poniewierski and R. Holyst, Phys. Rev. A **38**, 3721 (1988).
[2] A. Poniewierski, Phys. Rev. E **47**, 3396 (1993).
[3] Y. Mao, P. Bladon, H. N. W. Lekkerkerker, and M. E. Cates, Mol. Phys. **92**, 151 (1997).
[4] K. Yaman, P. Pincus, and C. M. Marques, Phys. Rev. Lett. **78**, 4514 (1997).
[5] B. Groh and S. Dietrich, Phys. Rev. E **59**, 4216 (1999).
[6] R. van Roij, M. Dijkstra, and R. Evans, Europhys. Lett. **49**, 350 (2000).
[7] R. van Roij, M. Dijkstra, and R. Evans, J. Chem. Phys. **113**, 7689 (2000).
[8] M. Dijkstra, R. van Roij, and R. Evans, Phys. Rev. E **63**, 051703 (2001).
[9] L. Onsager, Ann. N.Y. Acad. Sci. **51**, 627 (1949).
[10] A. B. D. Brown, S. M. Clarke, and A. R. Rennie, Langmuir **14**, 3129 (1998).
[11] F. M. van der Kroij and H. N. W. Lekkerkerker, J. Phys. Chem. B **102**, 7829 (1998).
[12] A. B. D. Brown, C. Ferrero, T. Narayanan, and A. R. Rennie, Eur. Phys. J. B **11**, 481 (1999).
[13] R. Evans, in *Fundamentals of Inhomogeneous Fluids*, edited by D. Henderson (Dekker, New York, 1992), p. 85.
[14] L. Harnau, D. Costa, and J.-P. Hansen, Europhys. Lett. **53**, 729 (2001).
[15] R. Eppenga and D. Frenkel, Mol. Phys. **52**, 1303 (1984).
[16] M. Dijkstra, J.-P. Hansen, and P. A. Madden, Phys. Rev. E **55**, 3044 (1997).
[17] M. A. Bates and D. Frenkel, J. Chem. Phys. **110**, 6553 (1999).
[18] F. van Swol and J. R. Henderson, Phys. Rev. A **40**, 2567 (1989).
[19] L. Lajtar, A. Patrykiejew, J. Penar, and S. Sokolowski, Chem. Phys. Lett. **139**, 277 (1987).